JOURNAL OF PROPULSION AND POWER
Vol. 9, No. 1, Jan.–Feb. 1993

Investigation of a Two-Dimensional Scramjet Inlet, $M_\infty = 8-18$ and $T_0 = 4100$ K

M. A. S. Minucci*
Instituto de Estudos Avançados—CTA, São José dos Campos, SP 12231-970, Brazil
and
H. T. Nagamatsu†
Rensselaer Polytechnic Institute, Troy, New York 12180

An investigation of a 25-cm span variable geometry two-dimensional scramjet inlet was conducted in the Rensselaer Polytechnic Institute (RPI) 0.61-m exit diameter nozzle hypersonic shock tunnel. During the tests the Mach number was varied from 8 to 18 and, for all runs, the stagnation conditions were approximately 5.5 MPa and 4100 K. The tests included surface and pitot pressure measurements of the internal hypersonic flow, as well as schlieren and air-luminosity photographs for flow visualization. The stagnation conditions were obtained by operating the helium driven hypersonic shock tunnel in the equilibrium interface mode. Useful test times of the order of 3–6 ms were obtained by this method. Due to the large Knudsen numbers, low pressure, and high stagnation temperatures present in the test section, the results indicated a very complex flow structure in the cowl region.

Nomenclature

A = function of the ratio of specific heats and wall temperature
a = speed of sound
F.S. = fuselage station measured from model leading edge
h = specific enthalpy
Kn = Knudsen number, λ/t
M = Mach number
N = number of intermolecular collisions
p = pressure
Re = Reynolds number
T = absolute temperature
t = leading-edge thickness or time
U = gas bulk velocity
V = molecular speed
Δ = interval
Θ = collision frequency, $N/\Delta t$
λ = mean free path
μ = viscosity
ξ = distance traversed due to the mass motion of the gas
ρ = density
χ = strong interaction parameter
$()_l$ = per unit length
$()_p$ = pitot pressure
$()_s$ = wall or shock conditions
$()_\infty$ = freestream conditions
$()_0$ = stagnation conditions
$()_1$ = driven tube initial conditions
$()_4$ = driver tube initial conditions
$()_5$ = reflected conditions
$()'$ = equilibrium interface conditions
$\bar{()}$ = mean value

Presented as Paper 91-0013 at the AIAA 29th Aerospace Sciences Meeting, Reno, NV, Jan. 7–10, 1991; received Aug. 5, 1991; revision received June 19, 1992; accepted for publication July 17, 1992.

*Captain, Brazilian Air Force. Member AIAA.
†Active Professor Emeritus of Aeronautical Engineering. Fellow AIAA.

Introduction

THE necessity of obtaining experimental data for the development of hypersonic air breathing vehicles such as the national aerospace plane (NASP, Mach = 25 and T_0 = 8000 K) and NASP derived vehicles (NDV) cannot be overstated.[1] Experimental results will provide not only the validation of the available CFD codes, but also the basic knowledge of the physics of the hypersonic flow phenomena.

The present study is actually a continuation of the authors' previous investigation[2] of the scramjet inlet flow when the stagnation temperature was kept below 1100 K. The same scramjet inlet model described in Ref. 2 was tested in the Mach number range from 8 to 18, and stagnation conditions of 5.5 MPa and 4100 K. Three additional pressure taps were installed so that additional pressure information could be obtained at critical stations. Also, in addition to the schlieren system used in the last investigation, one still camera and a video camera were included in the experimental setup so that air-luminosity photographs could be taken.

The tests were conducted in the RPI 0.61-m exit diameter nozzle hypersonic shock tunnel. The stagnation conditions were selected so that the real gas effects were present in the flow. These conditions, namely 5.5 MPa pressure and 4100 K temperature, correspond to the upper limit of the operational envelope of the facility and they were made possible through the operation of the shock tunnel in the equilibrium interface mode. In this mode of operation, higher pressures and temperatures than the reflected ones are generated after several shock reflections from the end wall and contact surface.[3,4] Useful test times of the order of 3–6 ms were attained for this particular mode of operation.

The Reynolds number range at the test section for the conditions stated above was 1.8×10^5 to 1.3×10^4 m^{-1} and the freestream Knudsen number varied from 1 to 31. Coincidentally, these conditions are very similar to those present in the experiments carried out by the senior author when investigating hypersonic flows over a flat plate.[5]

For the conditions described above, the results of this investigation indicated a very complex flow structure in the tested scramjet inlet.

Experimental Apparatus

RPI Hypersonic Shock Tunnel

The stainless steel driver and driven tubes are 4.6- and 16-m long, respectively, with a constant i.d. of 10.16 cm. In

all runs, the driven and driver initial pressures were respectively, 3.4 kPa (air) and 13.5 MPa (He) to produce a pressure ratio of 4000. Prior to loading the driven section, it was evacuated, flushed with dry high-purity air, and then pressurized to the desired final pressure. A 15-deg half-angle reflected-type conical nozzle[6] with an exit diameter of 0.61 m was used in the study. The flow Mach number in the test section can be changed simply by selecting the nozzle throat insert. A scored aluminum diaphragm, at the nozzle entrance, bursts with the arrival of the incident shock wave and the flow exhausts into a 5.7-m^3 pre-evacuated dump tank.

Three pressure transducers, installed upstream of the nozzle entrance, were used to trigger the data recording system, to pulse the schlieren light source, and to record the shock wave speed and the stagnation pressure history. One ionization gauge (described in Ref. 6) installed upstream of the nozzle inlet was used to indicate the presence of the ionized air at that location. At this same station, a RCA photodiode detector model C30807E was also used to indicate the duration of the high temperature airflow and the arrival of the contact surface.[3,4] Farther upstream of the nozzle entrance, two thin platinum heat transfer gauges[6] were used for additional information on the incident and reflected shock wave velocities, as well as to determine the propagation and spreading of the contact surface.[3,4] Two additional photodiodes, identical to the one described above, were used in the test section so that information on the start, duration, and end of the hot airflow past the model could be obtained. Figure 1 shows a schematic view of the relative location of the above-described instrumentation. In this figure, only the end part of the tunnel, including the nozzle and test section, is illustrated.

A second facility, a 18-m long 10.16-cm i.d. low-pressure shock tube is used to calibrate the pressure transducers installed in the model. A detailed description of the RPI hypersonic shock tunnel and shock tube is presented in Ref. 4.

Two-Dimensional Scramjet Inlet Model

In order to investigate the complex hypersonic flow in the scramjet, a 25-cm span, variable geometry two-dimensional scramjet inlet model was designed, built, and tested in the shock tunnel. Basically, it consists of two parallel wedges, the top one being adjustable vertically and horizontally. A schematic drawing of the model top and side views are shown in Fig. 2. According to this figure, surface pressure measurements are made along the model centerline at 11 different F.S.s. Four of them are located in the inlet ramp, three in the centerbody and the last four in the cowl. Relative distances of the pressure taps with respect to the model leading edge are also indicated in Fig. 2.

Pitot pressure measurements are made at two different F.S.s (Fig. 2). One of them is located at the inlet ramp leading-edge station. The second one is located near the cowl trailing

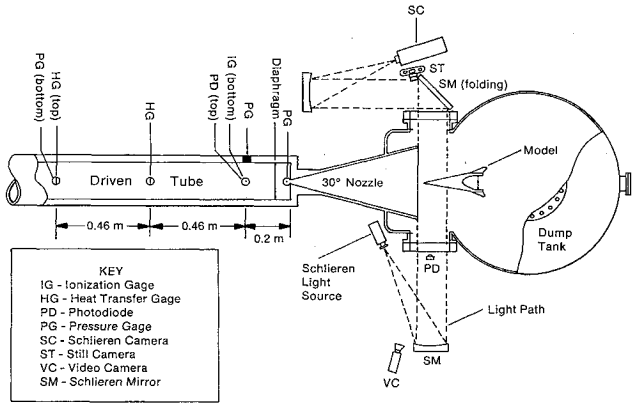

Fig. 1 Schematic view of the hypersonic shock tunnel instrumented section.

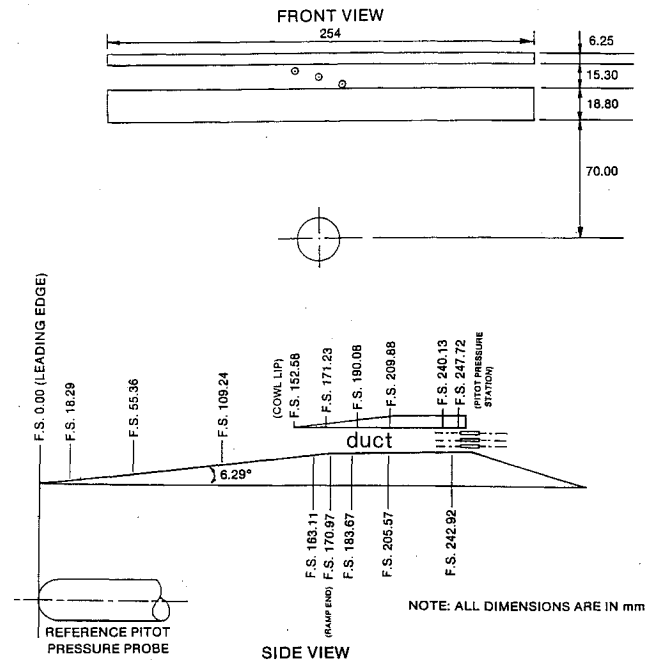

Fig. 2 Features of the scramjet inlet model tested.

edge. At this last station through the use of a three-probe rake, pitot pressure measurements are made simultaneously at three different heights from the centerbody surface.

The scramjet inlet model is mounted on two struts supported by a cart. The cart can be moved horizontally to properly position the model relatively to the nozzle exit. Electrical leads from the pressure gauges mounted in the model are brought out by means of a vacuum feed-through and connected to the data acquisition system.

Instrumentation

All pressures, both in the model and in the shock tunnel, are measured by piezoelectric pressure transducers. Prior to installation, the pressure transducers were dynamically calibrated in the low-pressure shock tube described previously. The gauges output, after amplification, are fed into a Tektronics Testlab 2520 data acquisition system and a Nicolet model 4094C digital oscilloscope.

Optical investigation of the flow over the model is made possible through the thick optically selected plate glass windows. A single pass schlieren arrangement was used to obtain the photographic records of the shock waves and the boundary layers whenever the flow conditions (density) permitted. The schlieren system uses a commercial spark gap as a light source. A convenient delay between the main trigger signal and light source is generated by a time delay generator. The purpose of the delay is to allow sufficient time for the flow establishment in the nozzle and over the model. Such delay time was experimentally found to be of the order of 3.5 ms.

Due to the high enthalpy stagnation conditions (6.5 MJ/kg), air becomes luminous over the model surfaces. Air luminosity photographs were taken simultaneously with the schlieren photographs through the use of a Cannon 35-mm still camera and a Sony 8-mm video camera. Some of the images obtained in this manner show very interesting information about the flow past the ramp inlet and the cowl region. Very often shock waves and boundary layers contours could be seen in the photographs obtained in this fashion even though they are a type of time-integrated photograph.[7] A schematic view of the optical recording set up can be seen in Fig. 1.

Test Conditions

As stated previously, the stagnation conditions used in this investigation are those obtained through the operation of the shock tunnel in the equilibrium interface mode.[3,4] Typical

shock-tube conditions are given in Table 1 and pressure and photodiode traces are shown in Fig. 3.

All values presented in Table 1 are experimentally determined with the exception of the reflected temperature T_5 and the equilibrium interface temperature T_5'. The reflected temperature is calculated as described in Refs. 3 and 4. On the other hand, T_5' is calculated assuming an isentropic compression of the gas from the reflected conditions P_5 and T_5 to the equilibrium interface conditions P_5' and T_5'.[3,4]

Values of relevant freestream flow parameters for selected shock-tunnel runs are presented in Table 2. The parameters given in this table assume reservoir conditions of 5.5 MPa and 4100 K which did not vary more than 5% from test to test. Most of the freestream flow properties listed in Table 2 were computed assuming an equilibrium expansion of the air in the nozzle. The validity of this assumption is based on previous results obtained during the nozzle calibration carried out by the senior author[8–10] under similar stagnation conditions (P_0 = 3.5 MPa, T_0 = 4000 K).

The NOZZLEFLOW code[4] uses as inputs the reservoir conditions P_0 and T_0, and the reference pitot pressure measured at the exit of the nozzle. The flow is assumed to be in equilibrium and real gas effects of air are introduced by the routines described in Ref. 11.

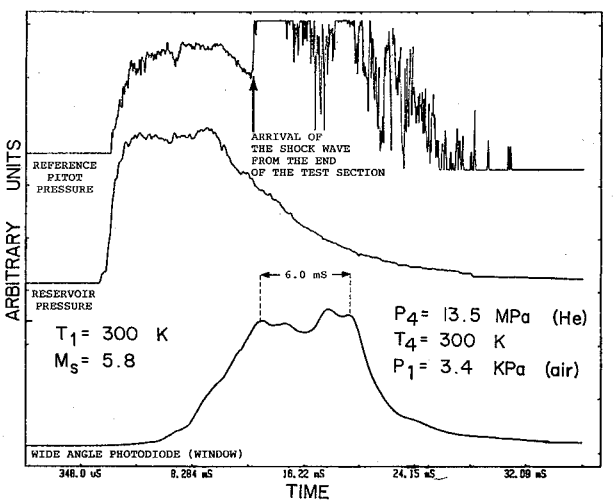

Fig. 3 Pressures and light emission measured during a real gas shock-tunnel run at the RPI facility.

Table 1 Typical shock-tube parameters

	Parameter	Value
Driver	Length	4.6 m
	Gas	Helium
	Pressure, p_4	13.5 MPa
	Temperature, T_4	300 K
Driven	Length	16 m
	Gas	Air
	Pressure, p_1	3.4 KPa
	Temperature, T_1	300 K
Shock Mach number, M_s		5.8
Reflected pressure, p_5		1.0 MPa
Reflected temperature, T_5		3300 K
Reservoir pressure, p_5'		5.5 MPa
Reservoir temperature, T_5'		4120 K
Reservoir enthalpy, h_5'		6.5 MJ/kg
Test time		3–6 ms

Table 2 Freestream conditions

M_∞	T_∞, K	p_∞, Pa	Kn_∞	$Re_{\infty,l}$, m^{-1}
8.0	447.0	157.0	1.11	1.7×10^5
10.0	296.0	37.0	2.80	8.3×10^4
12.0	208.0	11.0	6.10	4.6×10^4
15.0	135.0	2.4	15.0	2.3×10^4
18.0	94.3	0.68	31.0	1.4×10^4

Results and Discussion

As seen in Table 2, the Knudsen number based on the leading-edge thickness varies from 1 to 31, and very low Reynolds numbers are present for all tests. Figure 4 shows the variation of the mentioned parameters and additional ones as functions of the freestream Mach number.

The large Knudsen number variation indicates the large variation of flow regimes tested. These regimes range from small to very strong slip-flow effects due to the near free molecular flow experienced by the model at high Mach numbers. As first observed by Nagamatsu and Sheer[5] at high Knudsen numbers, the shock wave and the boundary-layer formation are delayed in forming at the very leading edge of the model. The region that preceeds the shock wave boundary-layer formation is known as a slip region. The slip region, as demonstrated by Nagamatsu and Sheer,[5,12] will increase linearly with the Mach number. Therefore, quite large slip distances can be expected at the highest Mach number tested, namely 18. As a matter of fact, the distance ξ_∞ traversed due to the mass motion of the gas for N intermolecular collisions can be found as follows: If Δt is the time required for N intermolecular collisions, and U_∞ is the bulk velocity of the gas one can write

$$\xi_\infty = U_\infty \Delta t \tag{1}$$

On the other hand, the freestream Mach number is defined as

$$M_\infty = U_\infty / a_\infty \tag{2}$$

Combining Eqs. (1) and (2) results in

$$\xi_\infty = a_\infty M_\infty \Delta t \tag{3}$$

Since the mean molecular speed is given by

$$\bar{V} = \theta \lambda_\infty \tag{4}$$

where $\theta = N/\Delta t$, one finally obtains from Eqs. (3) and (4)

$$\xi_\infty = (a_\infty / \bar{V}_\infty) N M_\infty \lambda_\infty \cong N M_\infty \lambda_\infty \tag{5}$$

As a consequence, the distance traveled by the molecules for one collision (N = 1) for the conditions present in the Mach 18 run will be 37 mm. Another important consequence

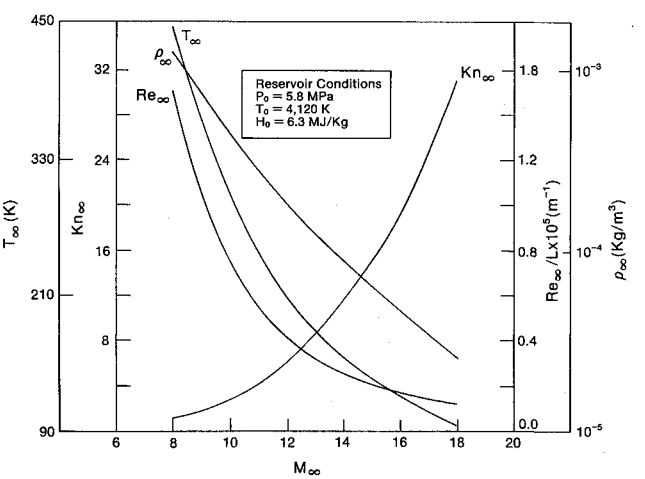

Fig. 4 Variation of the freestream parameters with the flow Mach number.

of this result is that the slip region over the inlet ramp will be considerably large and will strongly affect the flow in the cowl region.

By assuming the freestream viscosity to be a linear function of the temperature, the mean free path can be determined as[13]

$$\lambda_\infty = \mu_\infty/(0.499\rho_\infty \bar{V}_\infty) \tag{6}$$

Therefore, the freestream Reynolds number based on the leading-edge thickness can be written in terms of Kn_∞ as follows:

$$Re_\infty = (U_\infty/\bar{V}_\infty)(t/0.499\lambda_\infty) \cong (1/0.499)(M_\infty/Kn_\infty) \tag{7}$$

Therefore, as an important result the very large Knudsen numbers will indeed indicate a low Reynolds number flow. This result is confirmed by the values presented in Table 2 and in Fig. 4. The strength of the effects of the highly viscous flow over the model can be analyzed through the theory developed and experimentally verified by Nagamatsu and his associates.[14] According to this theory, for hypersonic Mach numbers, there is a region of noncontinuum flow (slip region, as discussed earlier) at the leading edge of a sharp flat plate. Such a region is followed by the formation of the shock wave and the viscous layer which are initially merged. This merged region is usually called the strong interaction region and is characterized by the freestream-based strong interaction parameter given by[15]

$$\chi_\infty = (M_\infty)^3 Re_\infty^{-1/2} \tag{8}$$

Downstream of this region, shock wave and boundary layer are separated by an inviscid layer and it is referred to as the "weak" interation region by Lees.[16]

Although the strong interaction region affects many flow parameters, the main objective of the present study is the measurements of the surface and pitot pressures. Therefore, only the viscous effects on the pressure will be considered.

To determine the effects of noninsulated flat plate on the hypersonic viscous interaction phenomena, Li and Nagamatsu[15] obtained the similar solutions of the compressible laminar boundary-layer equations and found that the hypersonic strong interaction with the surface pressure varying as $p_s/p_\infty \sim \chi_\infty^{-1/2}$ was a special case of the similar solution. As a result, Li and Nagamatsu[17] determined that the strong interaction effect on the pressure distribution on a flat plat is characterized by the following expression:

$$p_s/p_\infty = A\chi_\infty \tag{9}$$

where A is a function of the ratio of specific heats and the wall temperature ratio T_s/T_0 and its value can be found in Ref. 17. Equation (9) indicates that for the low Reynolds numbers present in the tests listed in Table 2 and Fig. 4, and mainly at the high Mach numbers, high pressures can be expected in the strong interaction region.

Another factor that will strongly influence the scramjet inlet flow is the flow chemistry itself. Due to the very low densities and high temperatures generated inside the viscous layer and behind the shock waves, the flow is not in equilibrium. Based on Nagamatu and Sheer's detailed boundary-layer profile surveys carried out on the low enthalpy hypersonic laminar boundary-layer on a 10-deg cone,[18,19] peak temperature can be expected to occur at about 20% of the boundary-layer thickness for a freestream Mach number of 14. At that location, the viscous flow moves at approximately 10% of the freestream Mach number and 40% of the freestream velocity. Additionally, the density is only 5% of the freestream value. Regardless of the fact that the surveys were conducted for stagnation temperatures of only 1400 K, this discussion indicates that the conditions for a nonequilibrium or frozen flow may exist in the present tests. Namely, the high speed (~1400 m/s), the high temperature (~4000 K) and the very low density could cause the flow to be either in local nonequilibrium or in a frozen state. Either one of the two situations will deviate the inlet pressure distribution from the one obtained by assuming equilibrium. Interestingly enough, current approaches to the NASP configuration[20] indicate that although bow shock waves are avoided, the slender compression inlet ramp will have to "live" with high temperature viscous layers. As a consequence, at high altitudes the same nonequilibrium/frozen effects discussed above may, likewise, be present. After the preceeding discussion on the factors influencing the scramjet inlet flow, a discussion of the results will be made.

Figure 5 shows schlieren photographs of the flow past the inlet ramp a) and past the centerbody b) at a flow Mach number of 8. Schlieren photographs of the flow Mach numbers of 10.0 and 12.0 were also obtained. However, they could not be reproduced due to their poor reproducibility. Due to the very low densities existing in the tests involving higher Mach numbers (15 and 18) no schlieren photographs were obtained. In Fig. 5a, the merged shock wave boundary-layer region is quite visible at the leading edge of the ramp (right side of the photograph). At Mach numbers 10 and 12, the very beginning of the shock wave was observed to be missing. Such a result is a consequence of the high Knudsen numbers causing a slip-flow region to exist at the leading edge. In Fig. 5b it is possible to observe the complex flow structure caused by the cowl shock wave ramp boundary-layer interaction. This flow structure was also present in the photographs obtained for the Mach 10 and 12 tests. Figure 6 shows a schematic of the flow pattern observed in Fig. 5b and at all flow Mach numbers investigated.

Figures 7 and 8 show air-luminosity photographs obtained at freestream Mach numbers of 12 and 15, respectively. In these figures it is possible to see the glowing boundary layer adjacent to the model surfaces. It is interesting to note that as the flow Mach number increases, the light intensity decreases. This observation is caused by the decrease in the freestream density. The background luminosity, as seen in Fig. 7, is caused by the stagnation region created at the end of the test section where the hypersonic flow comes to a dead

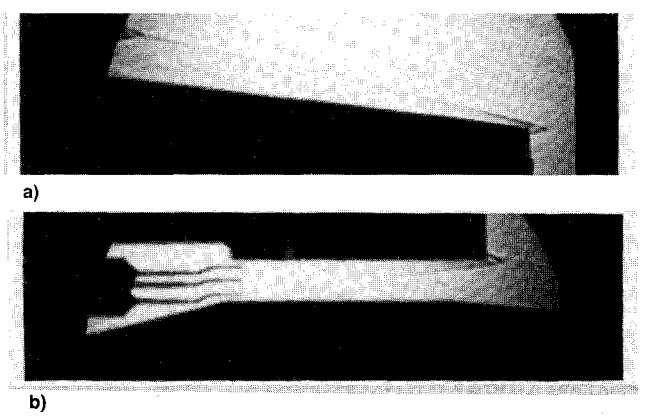

Fig. 5 Schlieren photographs of the Mach 8.0 flow a) past the ramp and b) in the cowl region (airflow is from right to left).

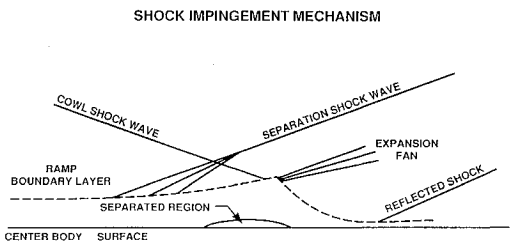

Fig. 6 Schematic of the shock wave boundary-layer interaction mechanism.

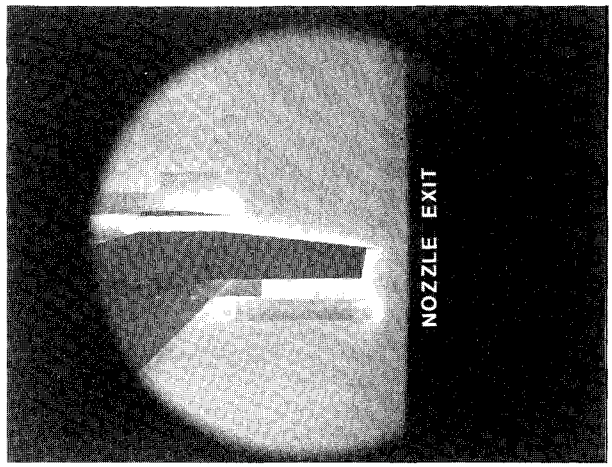

Fig. 7 Air-luminosity photograph of the Mach 12.0 flow over the scramjet inlet (airflow is from right to left).

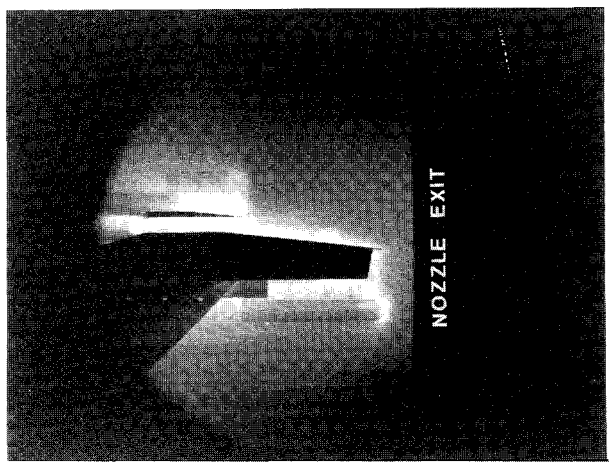

Fig. 8 Air-luminosity photograph of the Mach 15.0 flow over the scramjet inlet (airflow is from right to left).

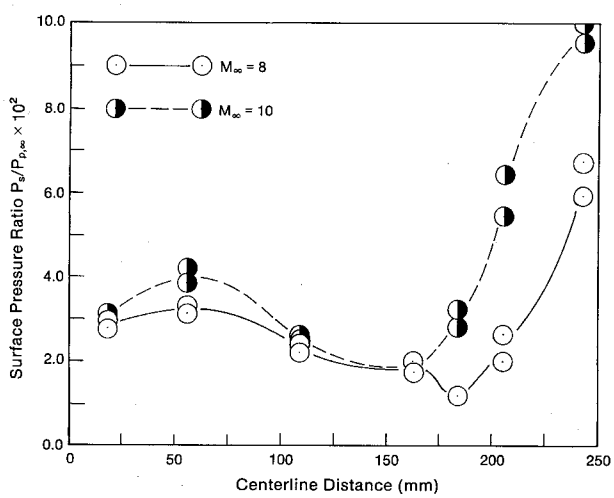

Fig. 9 Surface static pressures along the ramp centerbody centerline for the flow Mach numbers of 8.0 and 10.0.

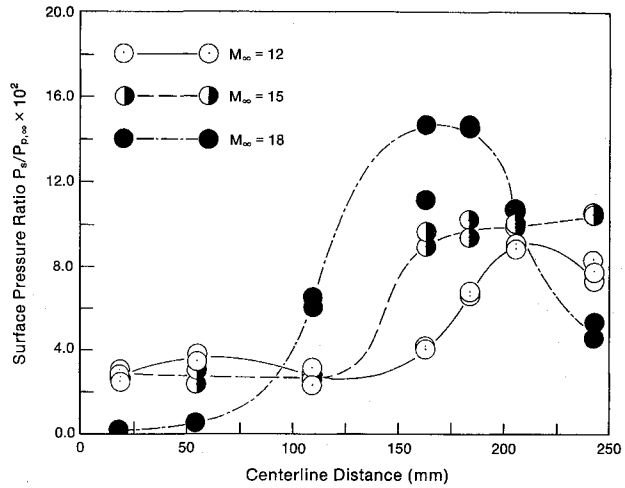

Fig. 10 Surface static pressures along the ramp centerbody centerline for the flow Mach numbers of 12.0, 15.0, and 18.0.

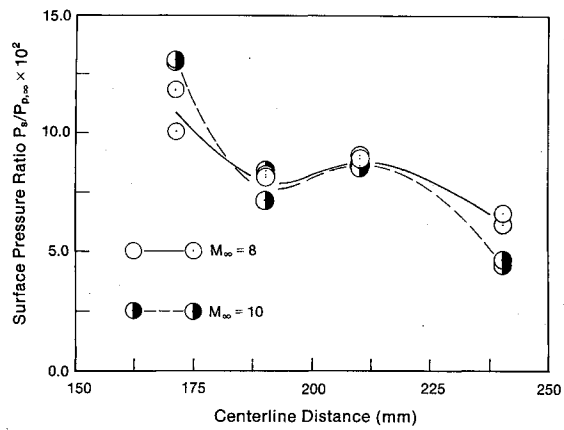

Fig. 11 Surface static pressures along the cowl centerline for the flow Mach numbers of 8.0 and 10.0.

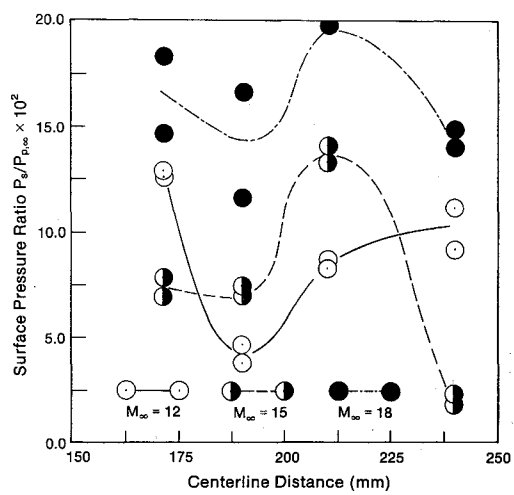

Fig. 12 Surface static pressures along the cowl centerline for the flow Mach numbers of 12.0, 15.0, and 18.0.

stop. Such luminosity is picked up by the wide-angle photodiode as shown in Fig. 4.

Figures 9–14 show the pressure measurements taken during the inlet tests. Multiple experimental points at the same F.S. represent results of separate shock-tunnel runs. The surface static pressure distributions along the ramp centerbody centerline are shown in Figs. 9 and 10. In these figures the centerline pressure p_s was nondimensionalized by the freestream pitot pressure $p_{p,\infty}$. In this way, the results presented contain only experimentally measured quantities. At Mach number 8 the pressure seems to increase close to the leading edge and then decreases at the end of the ramp. Due to the existence of an expansion (end of ramp and beginning of the centerbody) the pressure decreases at the entrance to the centerbody. As a consequence of cowl shock wave boundary-layer interactions, Figs. 5b and 6, the pressure increases in the aft portion of the duct. Except for the small pressure increase at the leading edge, this was the same trend observed when the

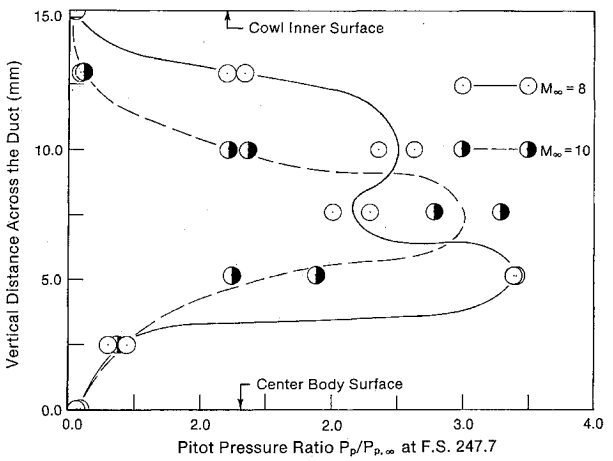

Fig. 13 Pitot pressure distributions at F.S. 247.7 for the flow Mach numbers of 8.0 and 10.0.

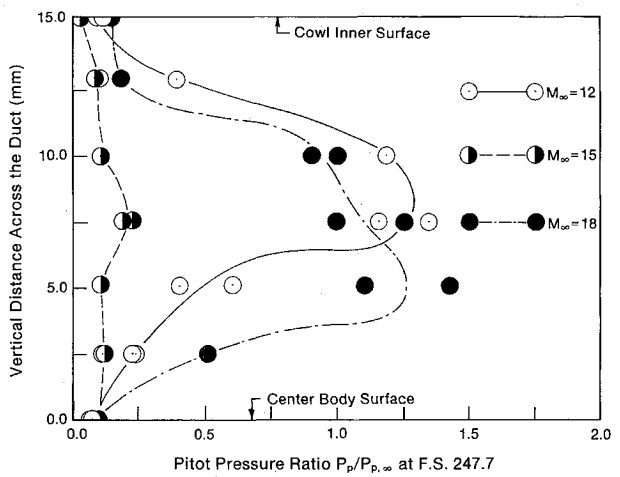

Fig. 14 Pitot pressure distributions at F.S. 247.7 for the flow Mach numbers of 12.0, 15.0, and 18.0.

stagnation temperature was lower (820 K) and the Knudsen number smaller (0.10).[2]

When the freestream Mach number is increased to 10, everything remains the same as for Mach 8, but the pressure does not decrease at the beginning of the centerbody. Somehow the internal flow does not "see" the turning at the end of the ramp. This is probably due to the growth of the separation region caused by the cowl shock wave impingement on the boundary layer (Figs. 5b and 6). In both cases (Mach numbers 8 and 10), the gradual increase in pressure at the ramp leading edge, instead of a sharp rise, as predicted by the strong interaction theory, can be explained on basis of the existence of a slip-flow region. At flow Mach number of 12, the surface pressure increases along the ramp centerline, followed by a steeper increase along the centerbody centerline. This last increase takes place only up to about half of the centerbody length. The second half of that region experiences a drop in pressure. An explanation for such pressure drop could be due to effects associated with the flow chemistry such as a sudden freezing. Air-luminosity photographs indicate the existence of very high temperatures in that region.

For a flow Mach number of 15, the surface pressure remains quite constant at the beginning of the ramp; after that, it continuously increases until a certain point inside the cowl region where it remains constant.

At the highest Mach number tested, namely 18, the pressure readings obtained at the two first pressure stations (close to the leading edge) show pressures very close to the freestream one (0.65 Pa). That is due to the very large freestream Knudsen number present which is 31. The two subsequent pressure readings along the centerline indicate a pressure increase at the end of the ramp. The first pressure station in the centerbody indicates about the same pressure as that in the previous region. The remaining two pressure stations show a very large drop in static surface pressure.

As a general trend, the peak pressure inside the cowl region seems to increase with the increasing flow Mach number. Such a trend was also observed for the scramjet inlet tests performed at low stagnation temperatures (777–1094 K) and smaller Knudsen numbers (0.10–0.92).[2] However, the decrease in the centerbody surface pressure observed in the present tests was never observed in the above-mentioned experiments.

Figures 11 and 12 show the variation of the cowl centerline surface pressures p_s. In a similar way as the two last figures, the surface pressures were made nondimensional by dividing them by the reference pitot pressure reading. At Mach numbers of 8 and 10, the trend is very similar to that observed in the low enthalpy runs.[2] For the higher Mach number cases though, the trend seems to be different. The peak surface pressures did not exist near the cowl leading edge. They seem to have been displaced towards the cowl trailing edge. This is a completely different behavior than that observed in the low stagnation temperature cases.[2] On the other hand, no matter where the high pressure location is, its value seems to increase with the increasing freestream Mach number.

Finally, the pitot pressure p_p distributions in the cowl region F.S. 247.7 are shown in Figs. 13 and 14. Again in these figures, the local pitot pressure was nondimensionalized by the freestream value. As a general rule, the pitot pressure decreases with the increasing flow Mach number. However the pitot pressure survey for Mach 18 shows much higher pressures than that for Mach 15. A similar feature was observed for the low enthalpy tests[2] when pitot pressures measured at the same location indicated a higher value for Mach 25 than for Mach 19. In these runs, schlieren photographs taken of the flow inside the cowl, for both Mach numbers, indicated that at Mach number 25 the duct was "cleared" due to a "smearing" of the shock waves and low densities. In the present investigation, the authors were not able to obtain schlieren photographs of the cowl flow at $M_\infty = 18$, but they believe the above to be also the explanation for the discussed observation.

Conclusions

An investigation of the internal flow in a two-dimensional variable geometry scramjet inlet was performed using the RPI 0.61-m diam hypersonic shock tunnel. The stagnation conditions investigated were 4100 K and 5.5 MPa with a corresponding stagnation enthalpy of 6.5 MJ/Kg. The selected freestream Mach numbers were 8, 10, 12, 15, and 18 corresponding to freestream Reynolds numbers of 1.8×10^5–1.3×10^4 m^{-1} range, and freestream Knudsen numbers in the 1–31 range.

Surface and pitot pressure measurements, along with schlieren and air-luminosity photographs, were made for the described flow conditions. The measurements indicate very complex flow structure due to the impingement of the cowl shock wave on the inlet ramp boundary layer. Also, the surface pressure measurements made near the ramp leading edge, indicate slip-flow effects due to the very large Knudsen numbers. Decreases in the high pressure centerbody region seem to indicate a possible local nonequilibrium or sudden freezing in the flow.

Pitot pressure measurements indicate high viscous losses in the cowl passage. An interesting observation is the higher pitot pressures existing in the duct region at Mach 18 than those measured at Mach 15. This is believed to be caused by the smearing of the shock waves and low densities existing in the duct.

Acknowledgments

The authors wish to acknowledge Watervliet Arsenal, Tektronics, Inc., PCB Piezotronics, and RCA—General Electric

for their technical support and donations. The authors also express their gratitude to L. N. Myrabo, R. Jones, F. Tesman, and C. Vannier for their effort to make this investigation possible. Finally, M. A. S. Minucci wishes to thank the Brazilian Air Force for supporting his Doctoral Program at the Rensselaer Polytechnic Institute.

References

[1]Gregory, T. J. "Credibility of NASP," *Aerospace America*, Vol. 27, No. 9, 1989, pp. 42–46.

[2]Minucci, M. A. S., and Nagamatsu, H. T., "Experimental Study of a Two-Dimensional Scramjet Inlet, M_∞ = 10.1–25.1," *Journal of Propulsion and Power*, Vol. 8, No. 3, 1992, pp. 680–686.

[3]Minucci, M. A. S., and Nagamatsu, H. T., "An Investigation of Hypersonic Shock Tunnel Testing at an Equilibrium Interface Condition of 4,100 K: Theory and Experiment," AIAA Paper 91-1707, Honolulu, HI, June 1991.

[4]Minucci, M. A. S., "An Experimental Investigation of a 2-D Scramjet Inlet at Flow Mach Numbers of 8 to 25 and Stagnation Temperatures of 800 to 4,100 K," Ph.D. Dissertation, Rensselaer Polytechnic Inst., Troy, NY, Aug. 1991.

[5]Nagamatsu, H. T., Geiger, R. E., and Sheer, R. E., Jr., "Hypersonic Shock Tunnel," *American Rocket Society Journal*, Vol. 29, No. 9, 1959, pp. 332–340.

[6]Nagamatsu, H. T., Sheer, R. E., Jr., and Schimid, J. R., "High Temperature Rarefied Hypersonic Flow over a Flat Plate," *American Rocket Society Journal*, Vol. 31, No. 7, 1961, pp. 902–910.

[7]Bloxom, D. E., Jr., "Supersonic Aerodynamic Experiments Using Very High Temperature Air Wind Tunnels," *Journal of Jet Propulsion*, Vol. 28, No. 9, 1958, pp. 603–609.

[8]Nagamatsu, H. T., Geiger, R. E., and Sheer, R. E., Jr., "Real Gas Effects in Flow over Blunt Bodies at Hypersonic Speeds," *Journal of the Aerospace Sciences*, Vol. 27, No. 4, 1960, pp. 241–251.

[9]Nagamatsu, H. T., Workman, J. B., and Sheer, R. E., Jr., Hypersonic Nozzle Expansion of Air with Atom Recombination Present," *Journal of the Aerospace Sciences*, Vol. 28, No. 11, 1961, pp. 833–837.

[10]Nagamatsu, H. T., and Sheer, R. E., Jr., "Vibrational Relaxation and Recombination of Nitrogen and Air in Hypersonic Nozzle Flows," *AIAA Journal*, Vol. 3, No. 1, 1960, pp. 1386–1391.

[11]Tannehill, J. C., and Mugge, P. H., "Improved Curve Fits for the Thermodynamic Properties of Equilibrium Air Suitable for Numerical Computation Using Time-Dependent or Shock-Capturing Methods," NASA CR-2470, Oct. 1974.

[12]Nagamatsu, H. T., and Li, T. Y., "Hypersonic Flow Near the Leading Edge of a Flat Plate," *Physics of Fluids Journal*, Vol. 3, No. 1, 1960, pp. 140–144.

[13]Kennard, E. H., *Kinetic Theory of Gases*, McGraw-Hill, New York, 1938.

[14]Li, T. Y., and Nagamatsu, H. T., "Shock-Wave Effects on the Laminar Skin Friction of an Insulated Flat Plate at Hypersonic Speeds," *Journal of the Aeronautical Sciences*, Vol. 20, No. 5, 1953, pp. 345–355.

[15]Li, T. Y., and Nagamatsu, H. T., "Similar Solutions of Compressible Boundary Layer Equations," *Journal of the Aeronautical Sciences*, Vol. 22, No. 9, 1955, pp. 607–616.

[16]Lees, L., "On Boundary Layer Equations in Hypersonic Flow and Their Approximate Solutions," *Journal of the Aeronautical Sciences*, Vol. 20, No. 2, 1953, p. 143.

[17]Li, T. Y., and Nagamatsu, H. T., "Hypersonic Viscous Flow on Noninsulated Flat Plate," *Proceedings of the Fourth Midwestern Conference on Fluid Mechanics*, Purdue Engineering Research Series, Purdue Univ., No. 128, Lafayette, IN, 1955, pp. 273–287.

[18]Nagamatsu, H. T., and Sheer, R. E., Jr., "Hypersonic Laminar Boundary-Layer Transition on 8-Foot Long, 10° Cone, M_1 = 9.1–16," *AIAA Journal*, Vol. 5, No. 7, 1967, pp. 1245–1251.

[19]Nagamatsu, H. T., and Sheer, R. E., Jr., "Critical Layer Concept Relative to Hypersonic Boundary Layer Stability," AIAA Paper 85-0303, Reno, NV, Jan. 1985.

[20]Anderson, J. D., Jr., *Hypersonic and High Temperature Gas Dynamics*, McGraw-Hill, New York, 1988, pp. 7–11.